Journal of Biomedical Optics 9(5), 995–1001 (September/October 2004)

# Blood cell counting and classification by nonflowing laser light scattering method

**Ye Yang**
**Zhenxi Zhang**
**Xinhui Yang**
Xi'an Jiaotong University
Institute of Biomedical Engineering
Xi'an 710049
China
E-mail: ye.yang@umassmed.edu

**Joon Hock Yeo**
Nanyang Technological University
School of MPE
Nanyang Avenue
Singapore 639798

**LiJun Jiang**
Institute for Infocom Research (I2R)
21 Heng Mui Keng Terrace
Singapore 119613

**Dazong Jiang**
Xi'an Jiaotong University
Institute of Biomedical Engineering
Xi'an 710049
China

**Abstract.** We present a nonflowing laser light scattering method for automatically counting and classifying blood cells. A linear charge-coupled device (CCD) and a silicon photoelectric cell (which is placed behind a pinhole plate on the CCD) form a double-detector structure: the CCD is used to detect the scattered light intensity distribution of the blood cells and the silicon photoelectric cell to complete the focusing process. An isotropic sphere, with relative refractivity near 1, is used to model the blood cell. Mie theory is used to describe the scattering of white blood cells and platelets, and anomalous diffraction, red blood cells. To obtain the size distribution of blood cells from their scattered light intensity distribution, the nonnegative constraint least-squares (NNLS) method combined with the Powell method and the precision punishment method are used. Both numerical simulation and experimental results are presented. This method can be used not only to measure the mean and the distribution of red blood cell size, but also to divide the white blood cells into three classes: lymphocytes, middle-sized cells, and neutrocytes. The experimental results show a linear relationship between the blood cell (both white and red blood cells) concentration and the scattered light intensity, and therefore, the number of blood cells in a unit volume can be determined from this relationship.  [DOI: 10.1117/1.1782572]

Keywords: blood cell; light scattering; counting and classification; charge-coupled device; nonflowing; cell sizing.

Paper 02091 received Dec. 30, 2002; revised manuscript received Nov. 11, 2003 and Jan. 8, 2004; accepted for publication Jan. 16, 2004.

## 1 Introduction

Blood cell counting and classification is one of the most commonly ordered clinical laboratory tests. It is a useful screening and diagnostic test often done as part of a routine physical examination. Blood cells can be divided into three types: red blood cells, white blood cells, and blood platelets. And their sizes, properties and functions are different. The diameter of a red blood cell is about 6 to 9 $\mu$m, and that of a white blood cell and blood platelet are 6 to 20 and 2 to 3 $\mu$m, respectively. There are mainly four methods for counting and classification of blood cells. The hemacytometer method,[1] a manual counting method, uses a counting chamber requiring checking under a microscopy. The photoelectric nephelometric method[1] can be used only to count normal red blood cells and results in large counting errors for abnormal cells. The other two available methods for blood cell counting and classification use either a Coulter counter[2,3] or a flow cytometer.[4–6] They measure a single cell flowing through the measuring region based on the electrical impedance (the so-called Coulter principle) or the laser scattering principle, respectively. But both have the common disadvantages of having complicated structures and high prices and they can easily be blocked due to the flow principle. Theera-Umpon and Gader used system-level trained neural networks to count white blood cells.[7] But training is a time-consuming process requiring the presentation of many white blood cell distributions to the neural network. To overcome these disadvantages, we present a new nonflowing laser light scattering method to count and classify blood cells, regarding blood cells as small particles. There have been many studies on particle size measurement using light scattering method,[8–15] digital imaging techniques,[16] the neural network technique,[17] photon migration techniques,[18] and the Coulter technique.[19] However, none of these techniques can be applied to all types of particles. Most of the research works on particle size measurement employing the light scattering method were based on the Fraunhofer diffraction theory or the Mie theory. They used general photoelectric detectors, multicircle photoelectric components,[9–13] or linear charge-coupled device (CCD) sensors[20] to detect the scattered light intensity of the particles. However, these methods have not been used in measuring blood cells and they could not provide information concerning the number of blood cells in a unit volume. To use the light scattering method for counting and classifying blood cells, the scattering properties of the blood cells must be studied, and a suitable inversion algorithm must be used to obtain the blood cell sizes and their distribution.

Address all correspondence to Ye Yang, University of Massachusetts Medical School. Tel: 508-792-1181; E-mail: ye.yang@umassmed.edu

1083-3668/2004/$15.00 © 2004 SPIE

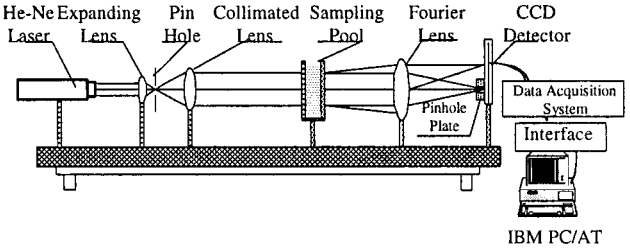


**Fig. 1** Schematic representation of the blood cell counting and classification experimental setup using the nonflowing laser light scattering method.

## 2 Experimental Setup and Working Principle

Figure 1 shows a schematic representation of the experimental set-up of the nonflowing laser light scattering method in our laboratory. In this system, the laser used is a 5-mW cw helium-neon (He-Ne) laser of wavelength 632.8 nm. The narrow He-Ne laser light that passed through a light-expanding lens, a pinhole filter, and a collimated lens was changed into a uniform wide parallel light. It was incident on a blood sample contained in a sampling pool and was scattered by the blood sample. The scattered light was collected by a linear CCD, which was positioned on the back focal plane of a Fourier lens, and was converted into an electric signal by the CCD. The analog electrical signal was converted into a digital signal and collected by a data acquisition system. Then the digital signal was transmitted to a computer through an interface circuit and was processed by the computer. The results of the blood cell size distribution, mean diameter, cell numbers, and white blood cell classification information can thus be obtained.

A linear CCD with 1024 elements (TCD132D, Toshiba Co., Japan) was used to detect the scattering light intensity distribution of the blood cells. It has the advantages of high sensitivity and high spatial resolution, but has the disadvantage that it is easily saturated. To overcome the disadvantage of the CCD and the difficulty of distinguishing the scattered light of blood cells from the nonscattered light at the light axis, a silicon photoelectric cell, which was positioned behind a pinhole plate on the CCD, was combined with the CCD to form a double-detector structure (Fig. 2) and was used to complete the focusing of the experimental setup. When the output of the silicon photoelectric cell reached maximum, the focusing process was completed.

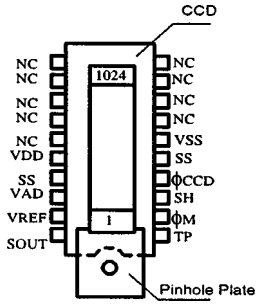


**Fig. 2** Schematic representation of a CCD combined with a pinhole plate as a double-detector structure. TP=test input, $\phi$M=master clock, SH=shift pulse, $\phi$CCD=CCD clock, SS=ground (analog), VSS=ground (digital), NC=non connection, SOUT=signal output, VREF=reference voltage input, VAD=power (analog), VDD=power (digital).

## 3 Theoretical Model and Analysis

### 3.1 *Theoretical Model*

Several theoretical models can be used to describe the light scattering of biological cells. The simplest model is a 2-D, opaque circular disk.[21] This model considers only the diffraction of light at the edge of the cell. A homogeneous sphere model[22] can describe the diffraction at the edge of the cell, and the reflection and refraction at the surface of the cell. But it cannot describe the influence of the cell nucleus. An opaque ring[23] can be used to account for the diffraction effects of the edges of the cell and the nucleus. A more realistic model for the biological cell would be a double-layered spherical structure, i.e., a sphere (nucleus) of one refractive index, surrounded by a coating (cytoplasm region) of another refractive index.[24] This theoretical model can represent the effects of the nuclear and cellular diffraction, refraction, reflection, and absorption, but its mathematical scattering description is very complex.

To describe the scattering of the blood cell and to avoid too much mathematical complexity, and as the relative refractivity of blood cell to water is near one,[25] we used an isotropic sphere with relative refractivity near one to simulate the blood cell.[26]

It is difficult to describe the scattering phenomenon by mathematical expressions. Until now, only the mathematical expressions of single scattering and elastic scattering have been studied.[27,28] There are many theories that can be used to describe the single and elastic scattering of various kinds of particles, such as the Fraunhofer diffraction theory, anomalous diffraction, the Rayleigh scattering theory, and the Mie theory.[27] Each theory's applicable scope is different. Mie theory can describe almost every kind of spherical particles, but it is very mathematically complicated. Fraunhofer diffraction theory does not consider the refractivity of the particle; it can be used to describe a large particle's diffraction. Rayleigh scattering can describe the scattering of a small particle with its size much smaller than the wavelength of the incident light. In some size ranges, the anomalous diffraction theory can be used to describe the scattering of a particle with refractivity near one. Blood cells can be considered as particles with size parameter $\alpha \gg 1$. Here $\alpha$ is a particle size parameter defined as $\alpha = \pi D/\lambda$, where $D$ is the diameter of the cell, and $\lambda$ is the wavelength of the light in the medium. As blood cells are large compared with the wavelength of the laser light we used, Rayleigh scattering theory is not applicable. From an investigation of the literature,[25] Fraunhofer diffraction is not suitable for red blood cells scattering since it does not consider the influence of the refractivity of the cells, and anomalous diffraction is suitable for them. This is in agreement with others[29–31] and our investigations.[26] Thus, anomalous diffraction was used for the red blood cells in this study, and Mie theory was used for the white blood cells and blood platelets. The relative refractivity of blood cells to the aqueous medium was assumed as $m = 1.04$, consistent with that assumed by other investigators.[32,33]

### 3.2 *Theoretical Analysis*

Only single scattering and elastic scattering are studied hereinafter. Let the intensity and wavelength in the medium of natural parallel light be, respectively, $I_0$ and $\lambda$ ($\lambda=\lambda_0/m$, where $\lambda_0$ is the light wavelength in the vacuum, and $m$ is the refractivity of the medium). When this light is incident on an isotropic spherical particle of diameter $D$, at the scattered angle $\theta$ in the CCD plane which is positioned on the back focal plane of the Fourier lens, whose focal length is $f$, the scattered light intensity $I(\theta)$ is[28]

$$I(\theta)=\left(\frac{\lambda}{2\pi f}\right)^2 I_0\left[\frac{i_1(m,\alpha,\theta)+i_2(m,\alpha,\theta)}{2}\right], \tag{1}$$

where $i_1$ and $i_2$ are the intensity functions whose mathematical descriptions for the Mie theory and the anomalous diffraction theory can be found in the literature;[27,28] $\alpha$ is the particle size parameter; $m=m_1-im_2$ is the particle refractivity in the medium, when the particle has absorption; and the image part $m_2$ of $m$ is not zero.

For a cell group whose number is $N$, if each cell has the same diameter, then in the condition of single scattering and elastic scattering, the total scattered light intensity is $N$ times that of a single cell. For multiple-sized cell dispersion, the total scattered light intensity is equal to the sum of the light intensity of single cell,[28] i.e.,

$$I(\theta)=I_0\int_0^\infty\left(\frac{\lambda}{2\pi f}\right)^2\frac{i_1+i_2}{2}f(D)\mathrm{d}D, \tag{2}$$

where $f(D)$ represents the number percentage of the cells in the range of some special size among the total cells.

As the cell volume percentage distribution $W(D)$ has the following relationship with the number percentage distribution $f(D)$:

$$f(D)=\frac{6}{\pi D^3}W(D). \tag{3}$$

Substituting Eq. (3) into Eq. (2), we can obtain

$$I(\theta)=I_0\int_0^\infty\frac{3\lambda^2}{4\pi^3D^3f^2}(i_1+i_2)W(D)\mathrm{d}D. \tag{4}$$

In fact, the size of every cell group to be measured is in some range ($D_{\min}$,$D_{\max}$), and the measuring of scattered light is also in some scattered range ($\theta_{\min}$,$\theta_{\max}$). In the case of forward scattering at small angles, there exists $\theta\cong r/f$, where $r$ is the distance between CCD sampling element and the light axis. Thus, $\theta$ is determined by the radial measuring range of the CCD ($r_{\min}$,$r_{\max}$) and $\theta_{\min}=r_{\min}/f$ and $\theta_{\max}=r_{\max}/f$. Then integral in Eq. (4) can be changed as sum form

$$\begin{aligned}I(\theta_i)&=I_0\int_{D_{\min}}^{D_{\max}}\frac{3\lambda^2}{4\pi^3D^3f^2}(i_1+i_2)W(D)\mathrm{d}D\\&=I_0\sum_{j=1}^{M}\frac{3\lambda^2}{4\pi^3D_j^3f^2}(i_1+i_2)W_j\quad i=1,2,\ldots,L,\end{aligned} \tag{5}$$

where $W_j$ is the volume percentage of the cells whose diameter is $D_j$ in the whole cells; $M$ is the number of the cell size ranges; $L=(r_{\max}-r_{\min})/\Delta r$ is the number of the sampling units of the CCD; and $\Delta r$ is the distance between each CCD sampling unit.

In Eq. (5), $I_0$ is a constant; we let it be 1. Equation (5) can be written in sample matrix form, i.e.,

$$\mathbf{I}=\mathbf{TW}, \tag{6}$$

where $\mathbf{I}=(I_1,I_2,\ldots,I_L)^T$ is the light intensity distribution vector, $\mathbf{W}=(W_1,W_2,\ldots,W_M)^T$ is the size distribution vector, and

$$\mathbf{T}=\begin{bmatrix}t_{1,1}&t_{1,2}&\cdots&t_{1,M}\\t_{2,1}&t_{2,2}&\cdots&t_{2,M}\\\vdots&&&\\t_{L,1}&t_{L,2}&&t_{L,M}\end{bmatrix}$$

is the light intensity distribution coefficient matrix. The elements of $\mathbf{T}$ are

$$t_{i,j}=\frac{3\lambda^2}{4\pi^3D_j^3f^2}\left[i_1\left(m,\frac{\pi D_j}{\lambda},\frac{r_i}{f}\right),i_2\left(m,\frac{\pi D_j}{\lambda},\frac{r_i}{f}\right)\right]. \tag{7}$$

The physical meaning of Eq. (7) is, with the position of the CCD a unit apart from the light axis $r_i$, the scattered light intensity caused by the cell of diameter $D_j$ is $t_{i,j}$. Equation (6) is the basic calculation equation of the nonflowing laser light scattering method.

Thus, when light distribution coefficient matrix $\mathbf{T}$ is known, either via the Mie theory or the anomalous scattering theory, we can use the CCD to detect the light intensity distribution vector $\mathbf{I}$ caused by the measured blood cells, then by solving the linear coupled equations $\mathbf{I}=\mathbf{TW}$ reasonably, we can acquire the distribution of the blood cell group size distribution. Due to the approximation of the principle, the influence of the coherent noise and the system noise, the ''ill-condition'' of the equation is almost inevitable, hence the usual methods used to solve the linear coupled equations cannot be applied to solve the distribution of blood cells. Also the distribution function we want to know has a constraint condition, i.e., each element of the size distribution should be nonnegative. The nonnegative constraint least squares (NNLS) method[34] is valid in solving the ill-conditioned linear coupled equations, but it has a problem of solution oscillation.[35] Twomey[35] pointed out that this problem can be ameliorated by adding another constraint condition, i.e., the solution vector should be smooth. By adding[35] a matrix $\mathbf{H}$ which makes the solution vector smooth, the solution of $\mathbf{W}$ can be reached when the next equation becomes minimum,

$$G=(\mathbf{TW}-\mathbf{I})^T(\mathbf{TW}-\mathbf{I})+\gamma\mathbf{WH}^T\mathbf{W}, \tag{8}$$

where $\gamma$ is the Lagrangian multiplier; i.e., to solve the NNLS problem of

$$\begin{cases}\|(\mathbf{T}^T\mathbf{T}+\gamma\mathbf{H})\mathbf{W}-\mathbf{T}^T\mathbf{T}\|_2=\min\\ \mathbf{W}\geqslant 0\end{cases}. \tag{9}$$

In Eq. (9), the choice of $\gamma$ is very important. When $\gamma=0$, the solved solution has a characteristic of violent oscillation. With the increasing of $\gamma$, the oscillation of the solved solution de-

**Table 1** Numerical simulation result of a three-peak distribution.

| Index | Size Range | Volume Fraction Set | Calculated Volume Fraction |
|---|---|---|---|
| 1 | 0.6–0.8 | 0 | 0 |
| 2 | 0.8–1.1 | 0 | 0 |
| 3 | 1.1–1.5 | 0 | 0 |
| 4 | 1.5–2.1 | 0.15 | 0.150262 |
| 5 | 2.1–2.9 | 0.20 | 0.200042 |
| 6 | 2.9–3.9 | 0 | 0 |
| 7 | 3.9–5.3 | 0 | 0 |
| 8 | 5.3–7.2 | 0 | 0 |
| 9 | 7.2–9.8 | 0.15 | 0.149734 |
| 10 | 9.8–13.3 | 0.25 | 0.249991 |
| 11 | 13.3–18.1 | 0.10 | 0.099982 |
| 12 | 18.1–24.6 | 0 | 0 |
| 13 | 24.6–33.4 | 0.05 | 0.050006 |
| 14 | 33.4–45.4 | 0.10 | 0.099983 |
| 15 | 45.4–61.7 | 0 | 0 |

creases. When the solved solution is a smooth curve, this solution can be regarded[35] as the solution of Eq. (6). But according to the view of Rizzi et al.[36] no matter what $\gamma$ is chosen, one still cannot make each component of the solution vector's error small. Thus, we present that after calculating by the NNLS method, we used the Powell method[37] and the precision punishment method[37] to calculate the solution vector again. Since the Powell method is accepted as the most effective method among the direct optimization methods, but it can only solve the nonconstraint optimization problem, we used the precision punishment method combined with it to solve the constraint optimization problem. The objective function changed as

$$P(x,v)=\sum_{i=1}^{L}(I_{ci}-I_{mi})^2+v\sum_{j=1}^{M}|\min(-W_j,0)|, \quad (10)$$

where $L$ is the number of the CCD sampling units; subscripts $c$ and $m$ represent the calculated and measured values of the light intensities, respectively; $I_{ci}$ represents the calculated light intensity value in the $i$'th detect unit; $I_{mi}$ represents the measured light intensity value detected by the $i$'th detect unit; $M$ is the number of the cell size ranges; $v$ is the punishment factor; and $W_j$ is the $j$'th component of the size distribution vector. By this method, we can make each component of the solution vector's error small, and the distribution of the cells can be solved by an independent model (by solving the distribution without assuming the blood cells fit to a special distribution). Numerical simulations and experimental results showed that this method can calculate the particle suspensions not only with a single-peak distribution, but also with double-peak and multipeak distribution accurately. Table 1 shows the numerical simulation result of a three-peak distribution. The size was divided into 15 classes (column 1) with different size ranges (column 2), and the volume fraction in each size class was set manually (column 3); in each simulation, a forward calculation with the exact size distribution generated the measured data. The calculated volume fraction in each size class under conditions of no noise using the presented algorithm is shown in the column 4 of Table 1. We can see that the three peaks set in the original size distribution can be reconstructed correctly.

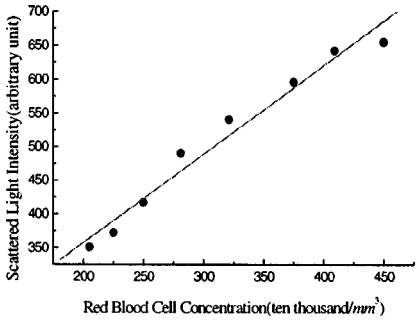


**Fig. 3** Dependence of the red blood cell concentration on the scattered light intensity.

## 4 Materials and Experiments

### 4.1 *Materials*

Some experiments of standard particles (polystyrene latex provided by Beijing Chemical and Metallurgy Research Institute) and human blood suspensions were measured at Xi'an Jiaotong Univerisity using the experimental measurement setup shown in Fig. 1. When measuring standard particles, the results fit well with the Coulter method results (all the standard particle's Coulter method results were provided by the standard particle provider). The standard deviation of the reproducibility of the setup was no more than 5%, and the system uncertainty was no more than 10%, compared with the nominal size of the standard particle.[26] The blood samples were randomly fetched from the donors at the Xi'an Jiaotong University Hospital Clinical Laboratory. The blood sample was heparin-anticoagulated venous blood. The number of male subjects was the same as that of female subjects. The donor ages were between 22 and 75. The blood diluents used in the experiments were the common diluents used by our university hospital, i.e., a red blood cell diluent of 0.9% saline and a white blood cell diluent of 3% acetum.

Using different quantities of blood cell diluents, the blood samples were diluted to different concentration of red blood cell suspensions and different concentration of white blood cell suspensions. Each sample's blood cell number was counted and the white blood cells were classified in advance by the hemacytometer method to compare with the results obtained by the presented method.

### 4.2 *Dependence of Blood Cell Concentration on Scattered Light Intensity*

The dependence of blood cell concentration on scattered light intensity was measured. The results are shown in Figs. 3 and

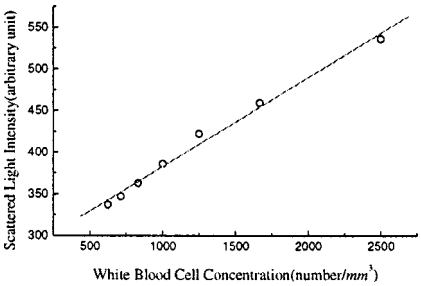


**Fig. 4** Dependence of the white blood cell concentration on the scattered light intensity.

4. The sum of the outputs of the first 50 pixels from the upper edge of the CCD (in the forward scattering direction) was defined as the scattering light intensity. As the scattering light intensities of the red blood cells were high, a variable neural density filter was used in front of the CCD when measuring red blood cells.

From Figs. 3 and 4, we can see that in some ranges of the red blood cell concentration, a linear relationship exists between the scattered light intensity and the red blood cell concentration. When the red blood cell concentration increased, the intensity of the scattered light also increased. In some ranges of white blood cell concentrations, a similar linear relationship also exists.

According to our measurements, when the concentrations of red blood cells increased over 800 ten thousand/mm$^3$, the curve showed an obviously nonlinear relationship. We considered that this was caused by the multiple scattering effect in the high concentrations. For white blood cells, this nonlinear threshold value was 11,000/mm$^3$. Typical values of red blood cell number and white blood cell number in 1 mm$^3$ are around 420 ten thousand to 620 ten thousand and 5,000 to 100,000 respectively,[1] so this nonlinearity will not influence the typical blood cell counting.

We consider the nonzero intercepts of the two fits in Figs. 3 and 4 were caused by the scattering of the particles in the saline or the red blood cell debris in the white blood cell diluent, when the concentration of red blood cells or white blood cells were zero (although we had subtracted the background scattering of cell diluent when measuring).

Currently, a qualitative linear relationship between the blood cell concentration and the light scattering intensity has been established. We found that the slope and offset of the curves shown in Figs. 3 and 4 vary from patient to patient. Further work to obtain a quantitative relationship by considering the gender and age and race of the donors is in progress.

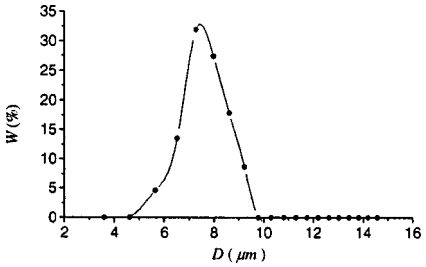


**Fig. 6** Red blood cell measurement result for subject 1.

### 4.3 *Measurement Results of Standard Particles*

Figure 5 shows the measurement result of a standard particle (polystyrene latex) aqueous suspension (the Coulter method's result was provided by the standard particle vendor). The result obtained from the presented method fits well with that from the Coulter method.

### 4.4 *Measurement Results of Blood Samples*

The size distribution of the red blood cell and white blood cells, and the mean diameter of the red blood cells were measured. The white blood cells were classified into three classes by measuring their size distribution. According to the literature,[38] the white blood cells between 4.67 and 7.6 $\mu$m can be counted as the lymphocytes (actually, lymphocyte are generally between 5.6 and 8.0 $\mu$m). And white blood cells with sizes between 7.6 and 10.1 $\mu$m can be regarded as middle-sized cells, which are mainly monocytes. But eosinophils, basophils, archecytes, and heterocytes are also in this range (7.6 to 10.7 $\mu$m). Thus, if the middle peak is exorbitant, we must pay attention to it, and take the manual hemacytometer result as the rule. The white blood cells of sizes 10.1 to 17.0 $\mu$m are regarded as neutrocytes. Thus, the white blood cells were classified as lymphocytes, neutrocytes, and middle-sized cells according to their size distribution. By this method, the small and large cell accordance ratio was high, and the accordance ratio of middle-sized cells was below 50%.

Figures 6 and 7 show one subject's (subject 1) red blood cell and white blood cell size distribution measurement results, respectively. The donor was a male of age 24. The counting result of the hemacytometer method was red cells number, 516 ten thousand/mm$^3$; lymphocytes 30%; and neu-

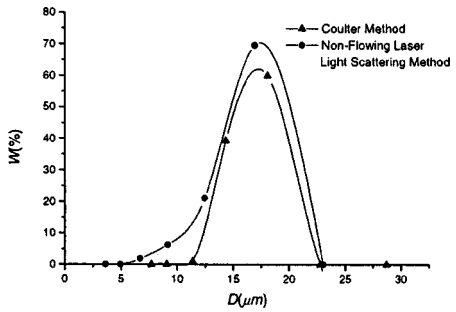


**Fig. 5** Measurement results of a standard particle with nominal diameter of 16.32 $\mu$m.

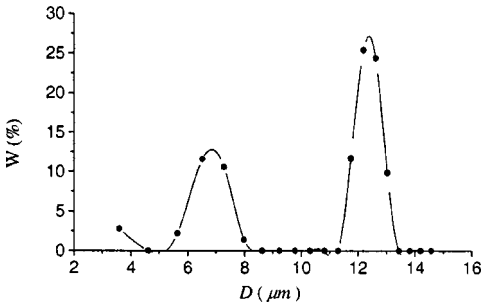


**Fig. 7** White blood cell measurement result for subject 1.

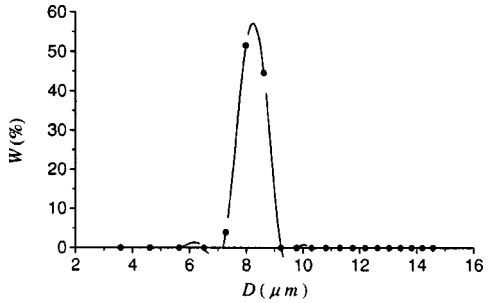


**Fig. 8** Red blood cell measurement result for subject 2.

trocyte 70%. The red blood cell mean diameter for this tester by the presented method was 7.69 $\mu$m. The result of the white blood cell classification by this method was lymphocytes, 25.1%; neutrocytes, 73.5%; and middle-sized cells, 1.4%.

Figures 8 and 9 shows another subject's (subject 2) red blood cell and white blood cell size distribution measurement results, respectively. The donor was a female of age 74. The counting result of the hemacytometer method was red cells number, 114 ten thousand/mm$^4$; lymphocytes, 27%; and neutrocytes, 72%; and monocytes, 1.0%. The red cell mean diameter for this tester by this method was 8.24 $\mu$m. It was greater than the normal value and implied that this patient may have anemia. The result of the white blood cell classification by the presented method was lymphocytes, 25.4%; neutrocytes, 61.7%; and middle-sized cells, 12.8%.

The measurement results fit well with the hemacytometer method. The mean diameters of the red blood cells in Figs. 6 and 8 have some discrepancy from the results reported in the literature[20,24] in which the mean diameter of a red blood cell as a homogeneous volume-equivalent sphere were determined as around 6 $\mu$m. We consider this discrepancy was caused by the difference between the subjects, since we do have some results derived from different subjects with mean diameters around 6 $\mu$m (data not shown here). Further work of comparing the presented method's results with those of other automatic methods such as the Coulter counter method will be processed.

## 5 Conclusions and Discussion

A new nonflowing laser light scattering method was presented here for counting and classifying blood cells automatically. A CCD and a silicon photoelectric cell (which was placed behind a pinhole plate on the CCD) formed a double-detector structure. The CCD was used to detect the scattered light intensity distribution of the blood cells, and the silicon photoelectric cell to complete the focusing of the experimental setup. An isotropic sphere with relative refractivity near 1 was used to model the blood cell. Mie theory was used to describe the scattering of white blood cells and platelets, and anomalous diffraction, red blood cells. Obtaining the size distribution of blood cells from their scattered light intensity distribution required the application of the NNLS method, the Powell method, and the precision punishment method. The experimental results showed that there is a linear relationship between the blood cell (white and red blood cells) concentration and the scattered light intensity. However, such relationships are varied in different gender, race, or age groups. Further work will be necessary to determine a general dependency of blood cell concentration on scattered light intensity, or different dependencies for different genders, ages, and racial groups, which would enable measuring the number of blood cells in a unit volume.

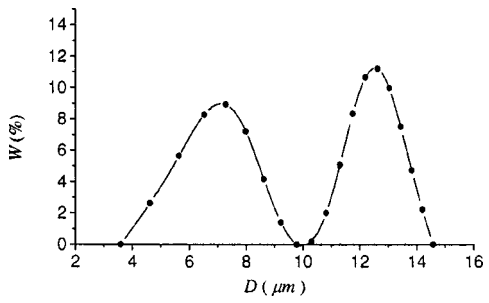


**Fig. 9** White blood cell measurement result for subject 2.

Our model assumes blood cells as homogeneous spheres of uniform refractive index for simplicity. In reality, cells are inhomogeneous and nonspherical in most situations, and their refractive indices are different. However, in a healthy human, the relative refractive index of the blood cells does not vary significantly.[25] It was also shown that, under certain conditions, forward light scattering by inhomogeneous particles can be amenable to an analytical treatment similar to that for uniform spherical particles.[39] On the other hand, modifications of the model, such as using ellipsoidal particles[25] or double-layered spherical structures,[24] should further improve the accuracy of the method. A refractive index can also be included as a parameter in the optimization procedure.

This method considers only single and elastic scattering and it is suitable for diluted suspension measurement *in vitro*. For *in vivo* measurement, where multiple scattering is present, some modification must be made to obtain an accurate value for matrix $\mathbf{T}$ in Eq. (6).

In summary, this paper presents an *in vitro* nonflowing laser light scattering method for automatically counting and classifying blood cells. It can be used (1) to determine the mean and distribution of the red blood cell size; (2) to divide the white blood cells into three classes according to their sizes, lymphocytes, middle-sized cells, and neutrocytes; and (3) to obtain the number of blood cells in a unit volume from the relationship between the blood cell concentration and the scattered light intensity.

### *Acknowledgments*

The authors would like to acknowledge the National Science Foundation of China (item number 60178034) for supporting this work.

### *References*

1. Q. Y. Li, M. Z. Xu, and X. Y. Kong, *Practical Clinical Medical Inspection*, Hu Bei People's Publish House, Wu Han (1980) (in Chinese).
2. T. Allen, *Particle Size Measurement*, pp. 455–478, Chapman and Hall, London (1990).
3. D. Chiappini, W. A. Wuillemin, M. Gardi, C. Jeanneret, and A. Tobler, "Comparability of haematology profile between QBC (R) autoread (TM) plus system and all electronic cell counting instrument

(Coulter Counter STKS),'' *Schweiz Med. Wochenschr* **130**(15), 545–550 (2000).
4. L. S. Cram, J. C. Martin, J. A. Steinkamp, T. M. Yoshida, T. N. Buican, B. L. Marrone, J. H. Jett, G. Salzman, and L. Sklar, ''New flow cytometric capabilities at the national flow cytometry resource,'' *Proc. IEEE* **80**(6), 912–917 (1992).
5. M. J. Dijkstra-Tiekstra, J. G. Schrijver, P. F. van der Meer, R. F. Laport, J. W. Gratama, W. H. Levering, and C. J. Van Delden, ''Crossover study of three methods for low-level white blood cell counting on two types of flow cytometer,'' *Cytom. Part B Clin. C. Y.* **54B**(1), 39–45 (2003).
6. F. S. Wang, Y. Itose, T. Tsuji, Y. Hamaguchi, K. Hirai, and T. Sakata, ''Development and clinical application of nucleated red blood cell counting and staging on the automated haematology analyser XE-2100(TM),'' *Clin. Lab Haematol.* **25**(1), 17–23 (2003).
7. N. Theera-Umpon and P. D. Gader, ''System-level training of neural networks for counting white blood cells,'' *IEEE Trans. Syst. Man Cybern.C* **32**(1), 48–53 (2002).
8. H. G. Barth, *Modern Methods of Particle Size Analysis*, Wiley, New York (1984).
9. R. A. Dobbins, L. Crocco, and I. Glassman, ''Measurement of mean particle sizes of sprays from diffractively scattered light,'' *AIAA J.* **1**(8), 1882–1886 (1963).
10. P. Latimer, ''Determination of diffractor size and shape from diffracted light,'' *Appl. Opt.* **17**(14), 2162–2170 (1978).
11. A. Boxman, H. G. Merkus, P. J. T. Verheijen, and B. Scarlett, ''Deconvolution of light-scattering patterns by observing intensity fluctuations,'' *Appl. Opt.* **30**(33), 4818–4823 (1991).
12. H. Schnablegger and O. Glatter, ''Optical sizing of small colloidal particles: an optimized regularization technique,'' *Appl. Opt.* **30**(33), 4889–4896 (1991).
13. J. H. Koo and E. D. Hirleman, ''Synthesis of integral transform solutions for the reconstruction of particle-size distributions from forward-scattered light,'' *Appl. Opt.* **31**(12), 2130–2140 (1992).
14. M. R. Jones, B. P. Curry, M. Q. Brewster, and K. H. Leong, ''Inversion of light-scattering measurements for particle size and optical constants: theoretical study,'' *Appl. Opt.* **33**(18), 4025–4034 (1994).
15. B. Ruck and B. Pavlovski, ''A new diffraction-based laser measuring principle for particle sizing,'' *Tech. Mess.* **70**(1), 25–37 (2003).
16. R. M. Carter and Y. Yan, ''On-line particle sizing of pulverized and granular fuels using digital imaging techniques,'' *Meas. Sci. Technol.* **14**(7), 1099–1109 (2003).
17. M. Z. Li, D. Wilkinson, and M. Schrodl, ''Neural network particle sizing in slurries by reflectance spectroscopy,'' *AIChE J.* **48**(11), 2492–2498 (2002).
18. M. Bartlett and H. B. Jiang, ''Particle sizing in dense, rapidly flowing KCl suspensions by photon migration techniques,'' *AIChE J.* **47**(1), 60–65 (2001).
19. G. H. McTainsh, A. W. Lynch, and R. Hales, ''Particle-size analysis of aeolian dusts, soils and sediments in very small quantities using a coulter multisizer,'' *Earth Surf. Processes Landforms* **22**(13), 1207–1216 (1997).
20. B. Schelinsky and H. Krambeer, ''Use of CCD sensors for two-dimensional optical particle sizing with an extended phase Doppler system,'' *Meas. Sci. Technol.* **14**(4), 500–507 (2003).
21. P. F. Mullaney and P. N. Dean, ''Cell sizing: a small-angle light-scattering method for sizing particles of low relative refractive index,'' *Appl. Opt.* **8**(11), 2361–2365 (1969).
22. A. Brunsting and P. F. Mullaney, ''Differential light scattering from spherical mammalian cells,'' *Biophys. J.* **14**, 439–446 (1974).
23. H. F. Tschunko, ''Annular apertures with high obstruction,'' *Appl. Opt.* **13**(1), 22–23 (1974).
24. M. Kerker, D. D. Cooke, H. Chew, and P. J. Mcnulty, ''Light scattering by structured spheres,'' *J. Opt. Soc. Am.* **68**(5), 592–601 (1978).
25. G. J. Streekstra, A. G. Hoekstra, E. J. Nijhof, and R. M. Heethaar, ''Light scattering by red blood cells in ektacytometry: Fraunhofer versus anomalous diffraction,'' *Appl. Opt.* **32**(13), 2266–2272 (1993).
26. Y. Yang, ''The study on blood cell counting and classification by stationary suspending laser light scattering method,'' PhD Dissertation, Xi'an Jiaotong University, Xi'an (1998) (in Chinese).
27. M. Kerker, *The Scattering of Light and Other Electromagnetic Radiation*, Academic, New York (1969).
28. H. C. Van de Hulst, *Light Scattering by Small Particles*, Dover, New York (1981).
29. A. G. Borovoi, E. I. Naats, and U. G. Oppel, ''Scattering of light by a red blood cell,'' *J. Biomed. Opt.* **3**(3), 364–372 (1998).
30. M. Hammer, D. Schweitzer, B. Michel, E. Thamm, and A. Kolb, ''Single scattering by red blood cells,'' *Appl. Opt.* **37**(31), 7410–7418 (1998).
31. J. M. Steinke and A. P. Shepherd, ''Comparison of Mie theory and the light scattering of red blood cells,'' *Appl. Opt.* **27**(19), 4027–4033 (1988).
32. A. N. Yaroslavsky, I. V. Yaroslavsky, T. Goldbach, and H. J. Schwarzmaier, ''Influence of the scattering phase function approximation on the optical properties of blood determined from the integrating sphere measurements,'' *J. Biomed. Opt.* **4**(1), 47–53 (1999).
33. P. F. Mullaney and P. N. Dean, ''The small angle light scattering of biological cells-theoretical considerations,'' *Biophys. J.* **10**(8), 764–772 (1970).
34. L. Huang, *The Linear Algebra in System and Control Theory*, Science Publish House, Bei Jing (1984) (in Chinese).
35. S. Twomey, *Introduction to the Mathematics of Inversion in Remote Sensing and Indirect Measurement*, Elsevier Scientific, New York (1977).
36. R. Rizzi, R. Guzzi, and R. Legnani, ''Aerosol size spectra from spectral extinction data: the use of a linear inversion method,'' *Appl. Opt.* **21**(9), 1578–1587 (1982).
37. R. Fletcher, *Practical Methods of Optimization*, Wiley, New York (1987).
38. X. H. Lu, ''Automatic blood cell analytical instruments,'' *Mod. Med. Instrum. Appl.* **6**(4), 12–16 (1994) (in Chinese).
39. Z. G. Chen, A. Taflove, and V. Backman, ''Equivalent volume-averaged light scattering behavior of randomly inhomogeneous dielectric spheres in the resonant range,'' *Opt. Lett.* **28**(10), 765–767 (2003).